Search for $B^+ \to K^+ \nu\bar{\nu}$ and other electroweak/radiative penguin processes at Belle II

Simon Kurz[a,*] **on behalf of the Belle II Collaboration**

[a]*Deutsches Elektronen-Synchrotron (DESY),*
Notkestrasse 85, 22607 Hamburg, Germany

E-mail: Simon.Kurz@desy.de

This contribution summarizes the first results from searches for electroweak and radiative penguin processes at the Belle II experiment installed at the SuperKEKB asymmetric energy electron-positron collider. The data sample considered by the analyses corresponds to an integrated luminosity of $63\,\mathrm{fb}^{-1}$ collected at the $\Upsilon(4S)$ resonance.

A brief summary of a search for $B \to X_s \gamma$ decays is given. This flavor-changing neutral-current decay is sensitive to many Standard Model extensions. An excess is clearly visible in the expected region.

The second result is a study of $B^\pm \to K^\pm \ell^+ \ell^-$ decays. This analysis will provide an independent measurement to shed more light onto the recently observed deviations from the Standard Model expectations. A preliminary measurement of the $B^\pm \to K^\pm \ell^+ \ell^-$ signal yield is discussed.

The main topic of this contribution is a search for the flavor-changing neutral-current decay $B^+ \to K^+ \nu\bar{\nu}$. A novel measurement method is developed, which exploits topological and kinematic properties of the decay that differ from both other B-meson decays and light-quark pair-production. This multivariate approach offers a significantly higher signal efficiency than the techniques used in previous publications. No signal is observed and an upper limit on the branching fraction of $B^+ \to K^+ \nu\bar{\nu}$ of 4.1×10^{-5} is set at the 90% confidence level.

*Speaker

1. Introduction

The Belle II experiment [1] is installed at the interaction region of the SuperKEKB collider [2], an asymmetric e^+e^- B meson factory, and its primary goal is to study CP-violation and rare decays. The center-of-mass energy of 10.58 GeV corresponds to the mass of the $\Upsilon(4S)$ resonance, which dominantly decays to a pair of B mesons. Belle II has recorded an integrated luminosity of 213 fb^{-1} so far but for the analyses presented in the following only 63 fb^{-1} have been analyzed. Furthermore, 9 fb^{-1} of so-called off-resonance data are used. These data are collected at an energy 60 MeV below the $\Upsilon(4S)$ resonance and only continuum events can occur (light-quark pair production or dilepton final states).

2. Observation of $B \to X_s \gamma$

The decay $B \to X_{(s,d)} \gamma$ involves the flavor-changing neutral-current process $b \to (s, d)\gamma$, which is sensitive to many potential Standard Model (SM) extensions. The goal of the analysis [3] is to measure the inclusive photon energy spectrum, where the process of interest produces a monoenergetic but smeared photon spectrum with an energy greater than 1.4 GeV. The analysis starts with the selection of a high energy photon and then applies simple selection requirements. A designated veto on photons from π^0 and η and multivariate analysis methods are implemented to suppress backgrounds. Comparing the data to the remaining background contributions, which are estimated using data-driven methods, an excess of events is clearly visible in the expected region as can be seen in Figure 1. A measurement with more data and improved analysis technique is in preparation.
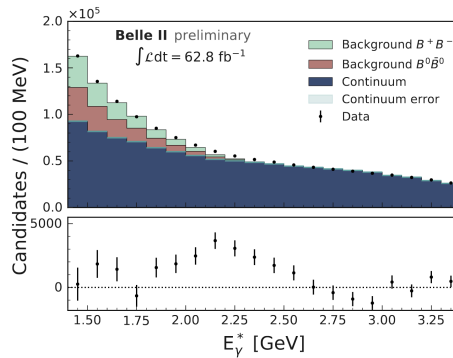

Figure 1: Photon energy spectrum of selected $b \to (s, d)\gamma$ candidates measured in the rest frame of the $\Upsilon(4S)$ event and the estimated background yields [3]. The lower plot shows the difference between observed number of events and the background expectations. Only statistical uncertainties are shown.

3. Study of $B^\pm \to K^\pm \ell^+ \ell^-$

For some years now, there has been a vivid interest in $B^\pm \to K^\pm \ell^+ \ell^-$ decays because deviations from the SM expectations are observed. A recent analysis by the LHCb collaboration [4] reveals even more evidence for the breaking of lepton universality in b-quark decays. Using 63 fb^{-1}

of data recorded by Belle II a preliminary measurement of the $B^{\pm} \to K^{\pm} \ell^+ \ell^-$ signal yield is performed [5]. The $B^{\pm} \to K^{\pm} \ell^+ \ell^-$ signal events are extracted by a two-dimensional fit in the beam-energy-constrained mass $M_{\text{bc}} = \sqrt{s/(4c^4) - (p_B^*)^2/c^2}$ and the variable $\Delta E = E_B^* - \sqrt{s}/2$, where $\sqrt{s}$ is the center-of-mass energy and E_B^* (p_B^*) correspond to the energy (momentum) of the non-signal B meson in the event, defined in the rest frame of the $\Upsilon(4S)$ system. A signal yield of $8.6^{+4.3}_{-3.9}$(stat.) ± 0.4(sys.) events is extracted. Signal-enhanced projections in both fit variables can be seen in Figure 2. The available data is not enough to determine interesting key observables like the branching fraction, the isospin asymmetry and the number R_K, given by the ratio of the branching ratios of the muon and electron decay channels. Instead, the full analysis is being prepared and validated using $B \to J/\psi(\to \ell^+ \ell^-)K$ (with $K = K^{\pm}, K_S^0$) control sample events, which have the same final state as the signal but a larger branching ratio.
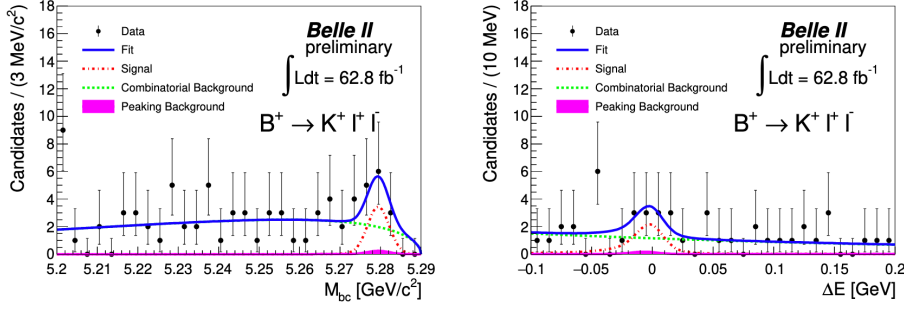

Figure 2: Signal-enhanced projection for a fit to the distributions of M_{bc} and ΔE of the selected $B^{\pm} \to K^{\pm} \ell^+ \ell^-$ signal candidate events. Details about the exact selection and the choice of fit functions can be found in [5].

4. Search for $B^+ \to K^+ \nu \bar{\nu}$

The main topic of this contribution is a search for $B^+ \to K^+ \nu \bar{\nu}$ events [6]. These flavor-changing neutral current transitions are a complementary probe of beyond the standard model (BSM) physics scenarios, which are proposed to explain the observed anomalies in $B^+ \to K^+ \ell^+ \ell^-$ transitions and which can be searched for with the available amount of data.[1] The $B^+ \to K^+ \nu \bar{\nu}$ process also has the advantage that it is not influenced by virtual photon contributions that complicate the theoretical calculations and could explain the observed anomalies. Figure 3 shows the leading-order Feynman diagrams for this process, which lead to the predicted branching fraction of $\mathcal{B}(B^+ \to K^+ \nu \bar{\nu}) = (4.6 \pm 0.5) \times 10^{-6}$ [7]. The process $B^+ \to K^+ \nu \bar{\nu}$ has not been observed yet but it is especially interesting to provide precise measurements as they help to constrain many BSM models like dark matter [8], leptoquarks [9] and axions [10].

Previous searches for this experimentally challenging decay explicitly reconstruct a semi-leptonic or hadronic decay of the non-signal B meson (B_{tag}) in the event, as indicated in Figure 4(a). These techniques suppress background very efficiently but inherently have a low signal efficiency, well below 1% ($\sim 0.2\%$ and $\sim 0.04\%$ for the semi-leptonic [11, 12] and hadronic [13–15] tags, respectively). In the presented search a novel and independent approach is developed inspired by

---

[1]Charge-conjugate channels are implied in the following.

(a) Penguin diagram   **(b)** Box diagram

Figure 3: Lowest-order quark-level diagrams for the $b \to s \nu \bar{\nu}$ transition in the SM [6].

Ref. [16], which exploits the distinct topology and kinematics of the signal events. With this method a higher signal efficiency of about 4% is achieved. Figure 4(b) illustrates that signal events typically exhibit distinct properties in comparison with background events. The $B^+ \to K^+ \nu \bar{\nu}$ events are more spherical than the jet-like continuum ($q\bar{q}$, $\tau\bar{\tau}$) events but less spherical than other, typical decays of B mesons. The neutrinos produced in the signal decay are observed as missing energy and make the event "unbalanced". Furthermore, the event includes a displaced track from the signal kaon.
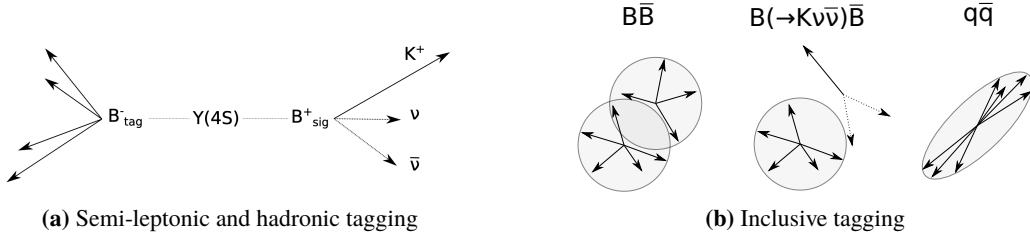

(a) Semi-leptonic and hadronic tagging   **(b)** Inclusive tagging

Figure 4: Semi-leptonic and hadronic tagging reconstruct the second B meson in the event (a), whereas inclusive tagging makes use of the distinct properties of the whole event (b).

In the first step of the analysis, events that consist of four to ten tracks are selected. To reject background events at a negligible loss of signal events, the total energy from all reconstructed charged and neutral particles in the event is required to exceed 4 GeV and the polar angle θ of the missing momentum must be between $17°$ and $160°$.

In the next step, the signal kaon candidate is selected. Since the signal track tends to have a higher momentum than background tracks, as is shown in Figure 5, the track with the highest transverse momentum that contains at least one hit in the pixel detector is chosen. The signal track is also required to be identified as a kaon.
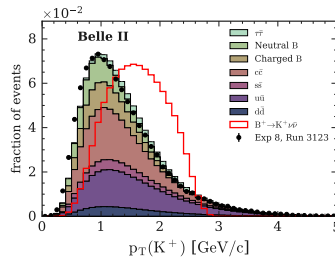

Figure 5: Distribution of the transverse momentum $p_T(K^+)$ of the signal kaon candidate track.

The core part of the analysis is a binary event classifier based on the FastBDT algorithm [17]. A large variety of variables that describe the topology and kinematics of the event, the properties of the rest-of-event, i.e. all particles but the signal kaon track, or the missing energy etc. have been investigated to distinguish signal from background events. Variables that provide little discrimination power or are poorly modeled in simulation are excluded and a set of 51 training variables is obtained. Three examples of selected training variables are given in Figure 6. The sphericity of signal events is typically in the intermediate range between continuum events at low values and more generic B meson events at high values. The Fox-Wolfram Moment R_1 describes the momentum imbalance in the event; the signal tends to have higher values due to the neutrinos. The variable ΔE of signal events tends to have lower values than for most of the background events. This variable is directly related to the rest-of-event, so in the case of signal events it is directly related to the non-signal B meson but for background events it is derived from random combination of objects from both B mesons.
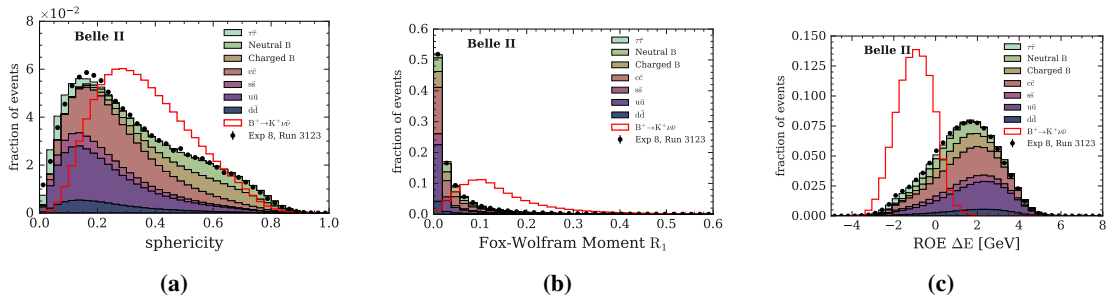

Figure 6: Distributions of the sphericity (a), the Fox-Wolfram Moment R_1 (b), and ΔE (c) that are used in the training of the event classifier.

To define the signal region a two-step procedure is implemented. A first binary classifier, BDT_1, is trained with the 51 variables. Then, all events with a classifier output of $\mathrm{BDT}_1 > 0.9$ are selected and a second classifier, BDT_2, is trained with a much larger sample and using the same 51 training variables. This procedure helps to keep the computational effort low, while significantly increasing the discrimination power. The highest signal sensitivity is achieved for $\mathrm{BDT}_2 \gtrsim 0.95$ as can be seen in Figure 7(a) at a signal efficiency of 4.3%. Based on this study 2×12 regions are defined in $\mathrm{BDT}_2 \times p_\mathrm{T}(K^+)$ space. Each of the 12 regions indicated in Figure 7(b) is defined in both on- and off-resonance data, which is important to constrain the background yields for the signal extraction.

It is especially important to validate the response of both BDTs in data and simulation. To that end, $B^+ \to K^+ J/\psi$ are selected in data and simulation. The J/ψ is reconstructed from two muons, which are then removed from the event to mimic the signal neutrinos. Furthermore, the momentum of the kaon candidate track is corrected using simulated signal events since $B^+ \to K^+ J/\psi$ consist of a two-body decay, whereas signal events are a three-body decay. The results of the study are summarized in Figure 8. The focus is on the red distributions marked with the label $J/\psi_{\to\mu^+\mu^-}$, which show the distributions of both event classifiers after the muon removal and the kinematic update for simulation and data. A high level of agreement can be seen for the distributions of the output of BDT_1 (main figure) and of BDT_2 (inset).
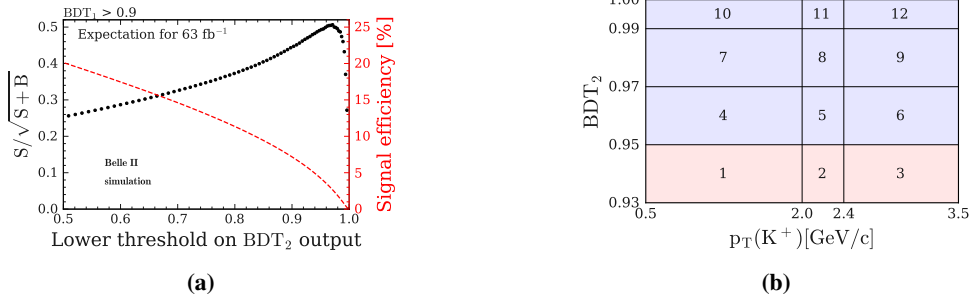
Figure 7: The signal sensitivity and signal efficiency as a function of the lower selection requirement on BDT_2 (a) and the derived two-dimensional search (blue) and control (red) regions.
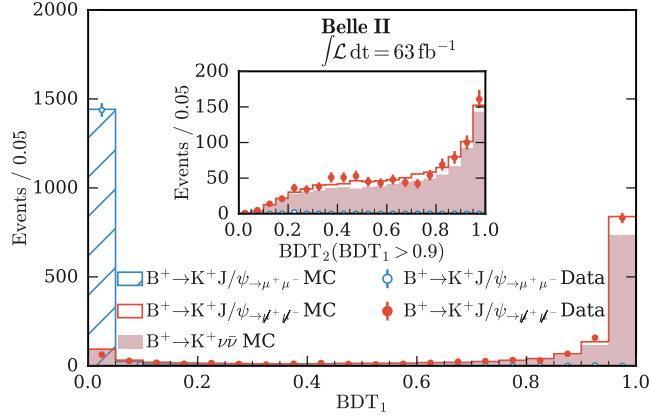

Figure 8: Results of the study to validate the output of both event classifiers [6]. The outer figure shows the distribution of the classifier output BDT_1 and the inset the distribution of BDT_2 for $BDT_1 > 0.9$.

To extract the signal yield a binned maximum likelihood fit is performed and the signal strength μ is determined, which is defined as a factor with respect to the SM expectation. Templates for signal and background yields are taken from simulation. Systematic uncertainties are included as nuisance parameters in the fit. The leading systematic is found to stem from the normalization of the individual background contributions. The yields obtained after the simultaneous fit of all 24 regions agree with the data as shown in Figure 9. The signal purity is found to be as high as 22% for the three tightest signal regions with $BDT_2 > 0.99$. The measured signal strength is $\mu = 4.2^{+2.9}_{-2.8}(\text{stat})^{+1.8}_{-1.6}(\text{syst})$.

As no signal is observed an upper limit is set on the branching ratio using the CL_s method [18]. The branching ratio is determined to be $\mathcal{B}(B^+ \to K^+ \nu\bar{\nu}) < (4.1 \pm 0.5) \times 10^{-5}$ at a 90% confidence level for a SM signal. For reinterpretation, the signal efficiency is given as a function of the invariant mass of the dineutrino system in Figure 10 (a).

As can be seen in Figure 10 (b), the measured branching ratio is compatible with previous publications. Since previous results are based on much larger data samples the presented result can be converted to the same luminosity assuming the total uncertainty on the branching fraction scales with the inverse square root of the integrated luminosity. This comparison reveals the presented
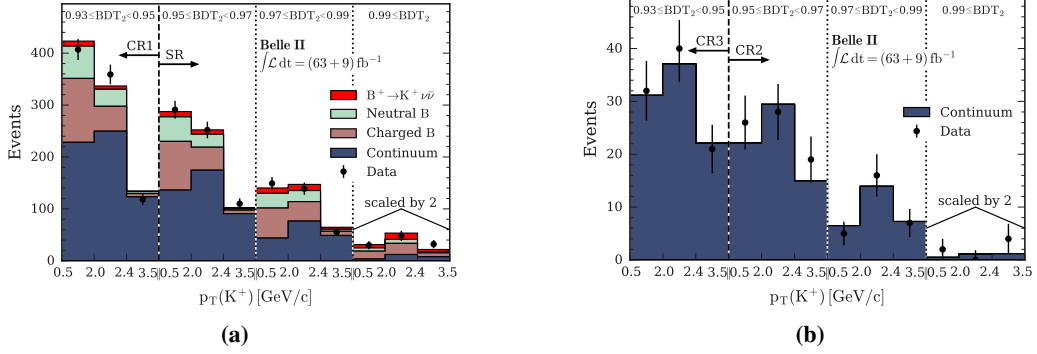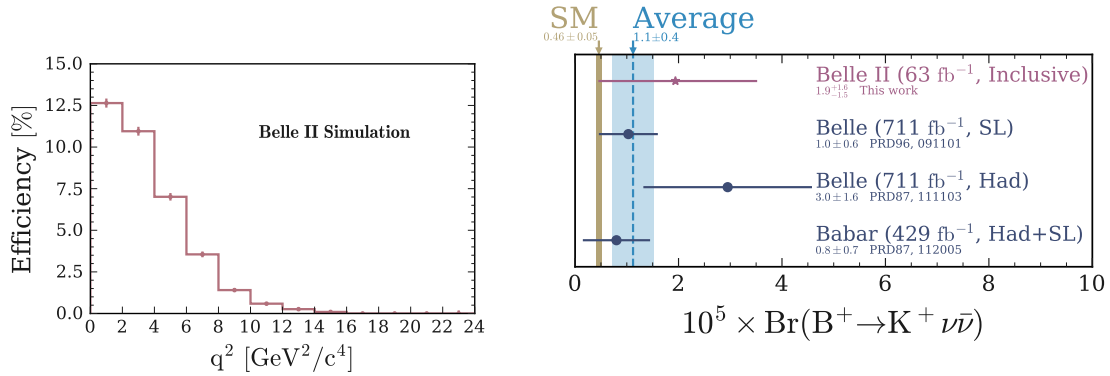
Figure 9: Yields in on-resonance data (a) and off-resonance data (b), in comparison to the expected yields estimated by the simultaneous fit to the on- and off-resonance data. All yields in the rightmost three bins are scaled by a factor of two.

analysis technique is better than semi-leptonic tagging by 10-20% and than hadronic tagging by a factor of 3.5.

(a) Signal efficiency as a function of the invariant mass of the dineutrino system q^2. The error bars indicate the statistical uncertainty.

(b) The branching ratio determined by the presented search (top), along with previous measurements. The brown and blue vertical bars illustrate the SM expectation and the average of all measurements, respectively.

Figure 10: Signal efficiency (a) and comparison of determined signal strength (b).

Due to the great performance of the inclusive tagging that is used to study the $B^+ \to K^+ \nu \bar{\nu}$ decays a follow-up analysis is already in preparation. It will use more data, include additional channels like $B^0 \to K^{*0} \nu \bar{\nu}$ and $B^0 \to K_S^0 \nu \bar{\nu}$, and an improved analysis technique. To further increase the signal sensitivity the results can be combined with measurements using semi-leptonic and hadronic tagging, which makes use of the fact that the obtained events are statistically independent.

5. Summary

These first few excellent results indicate the good performance of the still relatively new Belle II experiment, which show that Belle II is ready to look for new physics and make precision measurements of SM parameters. With the recent improvements in analysis techniques, previously unobserved processes like $B^+ \rightarrow K^+\nu\bar{\nu}$ may be observed for the first time very soon.

References

[1] Belle II Collaboration, "Belle II Technical Design Report", 2010, arXiv:1011.0352.

[2] SuperKEKB Collaboration, "SuperKEKB Collider", 2018, Nucl. Instrum. Meth. A **907**, 188.

[3] Belle II Collaboration, "Observation of inclusive $B \rightarrow X_s\gamma$ decays in early Phase III data (untagged)", 2021, BELLE2-NOTE-PL-2021-004.

[4] LHCb Collaboration, "Test of lepton universality in beauty-quark decays", 2021, submitted to Nature Physics, arXiv:2103.11769.

[5] Belle II Collaboration, "Study of $B^+ \rightarrow K^+\ell^+\ell^-$ at Belle II", 2021, BELLE2-NOTE-PL-2021-005.

[6] Belle II Collaboration, "Search for $B^+ \rightarrow K^+\nu\bar{\nu}$ decays using an inclusive tagging method at Belle II", 2021, arXiv:2104.12624.

[7] T. Blake, G. Lanfranchi, D. M. Straub, "Rare B Decays as Tests of the Standard Model", 2017, Prog. Part. Nucl. Phys. **92**, 50.

[8] A. Filimonova, R. Schäfer, S. Westhoff, "Probing dark sectors with long-lived particles at Belle II", 2020, Phys. Rev. D **101**, 095006.

[9] D. Bečirević, I. Doršner, S. Fajfer, D. A. Faroughy, N. Košnik, O. Sumensari, "Scalar leptoquarks from grand unified theories to accommodate the B-physics anomalies", 2018, Phys. Rev. D **98**, 055003.

[10] J. M. Camalich, M. Pospelov, P. N. H. Vuong, R. Ziegler, J. Zupan, "Quark Flavor Phenomenology of the QCD Axion", 2020, Phys. Rev. D **102**, 015023.

[11] BABAR Collaboration, "Search for the rare decay $B \rightarrow K\nu\bar{\nu}$", 2010, Phys. Rev. D **82**, 112002.

[12] Belle Collaboration, "Search for $B \rightarrow h\nu\bar{\nu}$ decays with semileptonic tagging at Belle", 2017, Phys. Rev. D **96**, 091101, [Addendum: 2018, Phys. Rev. D **97**, 099902].

[13] CLEO Collaboration, "Search for $B \rightarrow \tau\nu$ and $B \rightarrow K\nu\bar{\nu}$", 2001, Phys. Rev. Lett. **86**, 2950.

[14] Belle Collaboration, "Search for $B \rightarrow h^{(*)}\nu\bar{\nu}$ with the full Belle $\Upsilon(4S)$ data sample", 2013, Phys. Rev. D **87**, 111103.

[15] BABAR Collaboration, "Search for $B \rightarrow K^{(*)} \nu \bar{\nu}$ and invisible quarkonium decays", 2013, Phys. Rev. D **87**, 112005.

[16] Belle Collaboration, "Search for $B^+ \rightarrow \mu^+ \nu_\mu$ and $B^+ \rightarrow \mu^+ N$ with inclusive tagging", 2020, Phys. Rev. D **101**, 032007.

[17] T. Keck, "FastBDT: A Speed-Optimized Multivariate Classification Algorithm for the Belle II Experiment", 2017, Comput. Softw. Big Sci. **1**, 2.

[18] A. L. Read, "Presentation of search results: the CL$_s$ technique", 2002, J. Phys. G: Nucl. Part. Phys. **28**, 2693.